2.6 Constraining the CKM Matrix

2.6.1 Introduction

The study of particles containing the bottom quark has provided valuable insights into the weak interactions and QCD: *e.g.* the long lifetime of b hadrons, the large mixing observed in the B^0–$\bar{B}^0$ system, the discovery of heavy quark symmetries and the utility of heavy quark effective theories, the observation of "penguin" decays. This is not surprising given that the bottom quark is heavy and that its preferred charged current coupling to the top quark occurs only in virtual higher–order processes. The b hadrons provide a valuable laboratory in which to extract fundamental parameters of the Standard Model and test its consistency and search for rare processes which are sensitive to physics beyond the Standard Model.

Measurements with b hadrons can in principle be used to extract information on 5 of the 9 elements of the CKM matrix that relates the weak–interaction and mass eigenstates of quarks. The CKM matrix can be written as:

$$V = \begin{pmatrix} V_{ud} & V_{us} & V_{ub} \\ V_{cd} & V_{cs} & V_{cb} \\ V_{td} & V_{ts} & V_{tb} \end{pmatrix} \tag{2.2}$$

or in the Wolfenstein [1] parameterization:

$$\simeq \begin{pmatrix} 1-\lambda^2/2 & \lambda & A\lambda^3(\rho - i\eta) \\ -\lambda & 1-\lambda^2/2 & A\lambda^2 \\ A\lambda^3(1-\rho-i\eta) & -A\lambda^2 & 1 \end{pmatrix} \tag{2.3}$$

given here to $O(\lambda^4)$, where $\lambda = \sin(\theta_{\mathrm{Cabibbo}})$ and the other three parameters A, ρ, and η encode the remaining two weak mixing angles and the irreducible complex phase that introduces *CP* violation.

Unitarity of the CKM matrix requires the relationship

$$V^*_{tb}V_{td} + V^*_{cb}V_{cd} + V^*_{ub}V_{ud} = 0, \tag{2.4}$$

which can be displayed as a triangle in the complex plane, as shown in Figure 2.56. The base of this triangle has been rescaled by $A\lambda^3$ to be of unit length. Also shown are the angles α, β, and γ which lead to *CP* violating effects (provided the triangle does not collapse to a line) that can, in principle, be measured with b hadrons.

The b physics goals for CDF II include:

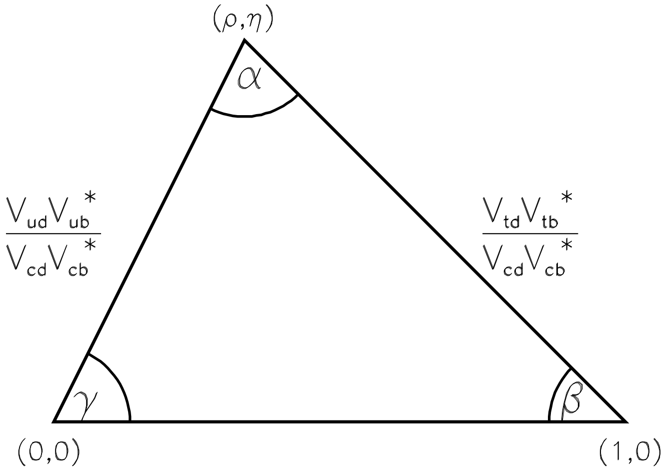

Figure 2.56: The unitarity triangle indicating the relationship between the CKM elements.

- An observation of *CP* violation in $B^0 \to J/\psi K^0_S$ and a measurement of $\sin(2\beta)$ with a precision comparable to e^+e^- machines
- An observation of *CP* violation in $B^0 \to \pi^+\pi^-$ and a measurement of $\sin(2\alpha)$ to ± 0.10
- Determination of $|V_{td}/V_{ts}|$ with a precision of 20% over the full range allowed by the Standard Model

The copious production of b hadrons of several species at the Tevatron offers the opportunity to provide measurements that will allow us to fully check the consistency of the CKM picture. To take advantage of the broad spectrum and high rate of production of b hadrons at the Tevatron, the challenges of triggering and event reconstruction in high energy $p\bar{p}$ collisions must be successfully met.

2.6.2 The current CDF b program

CDF has demonstrated the ability to mount a b physics program exploiting the unique aspects of hadron production. Approximately twenty papers have been published (or are submitted and under review) in PRL and PRD by CDF on the subject. Many of the CDF results are highly competitive with measurements from LEP or CLEO and some of them are the best measurements from a single experiment. These measurements include:

- Individual b hadron masses (B^+, B^0, B_s, Λ_b) [2, 3]
- Individual b hadron lifetimes (B^+, B^0, B_s, Λ_b) [4, 5, 6]
- Polarization in $B^0 \rightarrow J/\psi K^{*0}$ and $B_s \rightarrow J/\psi\phi$ [7]
- Search for $B_c \rightarrow J/\psi\pi$ [8]
- Searches for rare decays ($B^0, B_s \rightarrow \mu^+\mu^-$; $B^\pm \rightarrow \mu\mu K^\pm$; $B^0 \rightarrow \mu\mu K^{*0}$; $B^0, B_s \rightarrow \mu e$) [9]

There are other physics topics for which CDF has preliminary results based on Run Ia data (≈ 20 pb^{-1}). These ongoing analyses will also be competitive with LEP and CESR with the full Run I data set (≈ 110 pb^{-1}) and include: a measurement of the B_d mixing parameter x_d, limits on the B_s mixing parameter x_s, measurement of the ratio of branching ratios for color–suppressed B meson decays, and a search for $B_c \rightarrow J/\psi\ell\nu$.

CDF has also carried out several studies of B and quarkonium production and of $b\bar{b}$ production correlations [10, 11]. The QCD aspects of these results have generated much interest. In addition, they provide the understanding of B production necessary for studies of B decay.

The analyses carried out by CDF have shown that the mass resolution obtained with the CTC coupled with the vertex resolution obtained with the SVX allows us to (a) isolate fully–reconstructed B decays and (b) measure the lifetime of the decaying mesons. Point (a) is illustrated in Figure 2.57 where the observed signals for $B^\pm \rightarrow J/\psi K^\pm$ and $B^0 \rightarrow J/\psi K^{*0}$ are displayed. These data samples are currently the world's largest for these decay modes. Point (b) is illustrated in Figure 2.58 where the lifetime distribution for exclusive $B \rightarrow \psi K$ modes is used to extract the individual $B^\pm$ and B^0 meson lifetimes.

In addition, we have gained considerable experience in measuring the B decay vertex in partially reconstructed B semileptonic decays. For example, we have used the decays $B^- \rightarrow \ell^- D^0 \bar{\nu}$ and $B^0 \rightarrow \ell^- D^{*+} \bar{\nu}$ to measure the lifetimes of the charged and neutral B mesons. The D meson signals are displayed in Figure 2.59, and the corresponding B lifetime distributions are displayed in Figure 2.60. Note that these measurements do not rely on the presence of a J/ψ in the final state for triggering or reconstruction purposes. These results (and similar ones shown later for B_s decays) demonstrate the ability to measure B lifetimes in decays involving two secondary vertices (one due to the B decay and one due to the D decay).

By combining our Run I results using exclusive decays and semileptonic decays, we obtain a ratio of the B^+ to B^0 lifetimes of 1.09 ± 0.05. Figure 2.61 graphically compares CDF's results on b hadron lifetimes with the combined results of the LEP experiments (from the 1995 Lepton Photon Symposium).

Currently, CDF is unique in having a sample of $B \rightarrow J/\psi K_S$ events that can be tagged for a *CP* asymmetry analysis. We are working on several flavor tagging methods and expect to apply these methods to a first study of the *CP* asymmetry using the Run I data.

2.6.3 CDF II strategy for b physics

The current generation of B experiments, CDF, CLEO, LEP and SLD, are already making important measurements and placing constraints on the parameters of the CKM matrix. On the time scale of Run II, there will be competition among many new or upgraded experiments. CDF II will take advantage of the broad spectrum of b hadrons produced at the Tevatron which makes measurements with B_s, B_c and b baryons as well as with B^0 and B^+ possible. Key elements of CDF that made the Run I high–p_T physics program (*e.g.* top and W) so successful include excellent tracking resolution, lepton identification (including dE/dx), secondary–vertex reconstruction and a flexible and powerful trigger and data acquisition system. These same elements are also the foundation upon which a successful b physics program has been built.

The strategy for CDF II is to build on our experience in Run I, to optimize the quality of information in the central region while expanding coverage, and to exploit many additional b hadron decay channels. The tracking upgrades (SVXII/ISL/COT) are expected to improve the present mass resolution while the 3D silicon tracker (SVXII) is expected to improve the vertex finding ability. The lepton and tracking coverage will be increased (SVXII, ISL and CMX/IMU). The dE/dx information from the COT will be employed for particle identification. In CDF II we also plan to leave sufficient space at the outer diameter of the tracking volume (COT) for a Time–of–Flight system designed to provide for K/π separation

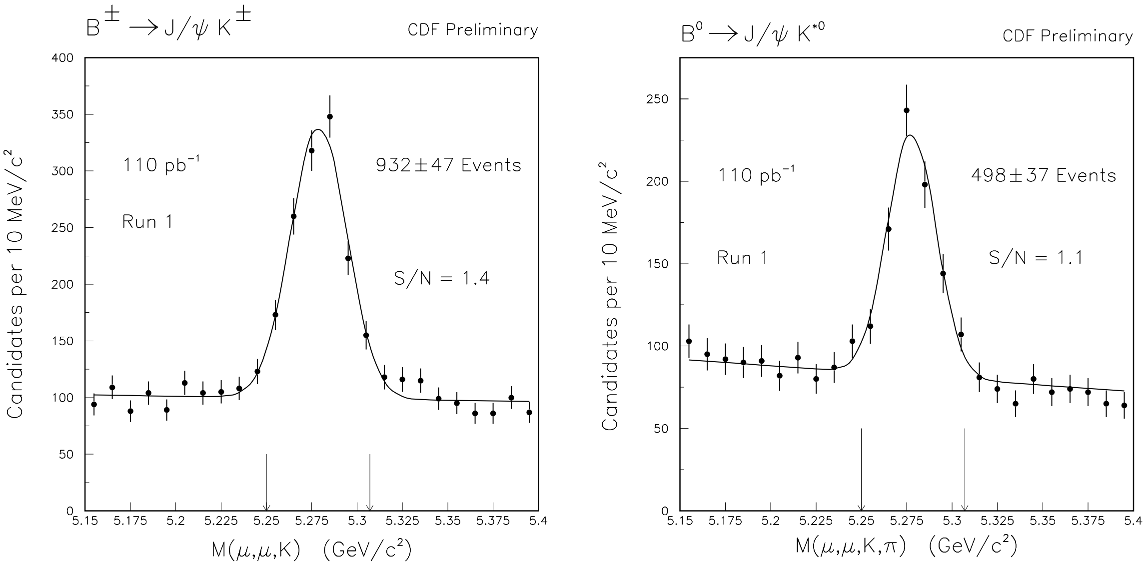

Figure 2.57: The invariant mass distributions for charged and neutral B mesons reconstructed via the decay modes $B^+ \to J/\psi K^+$ and $B^0 \to J/\psi K^{*0}$ as observed by CDF.

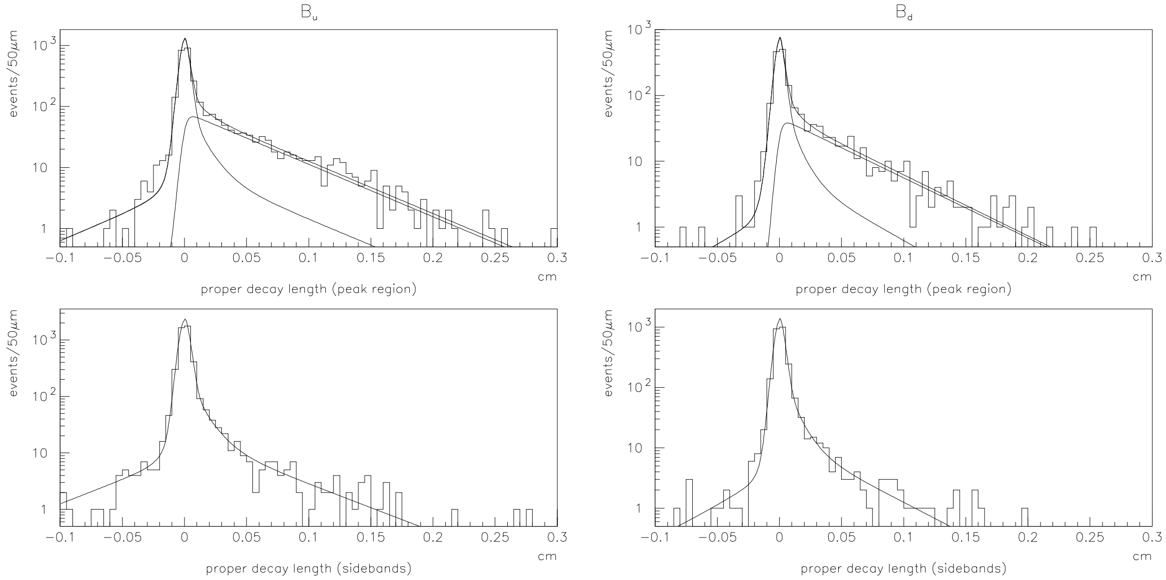

Figure 2.58: The proper lifetime distributions for charged and neutral B mesons reconstructed via the exclusive $B \to \psi K$ decay modes are shown in the upper plots. The lower plots display the background distributions for the B sidebands.

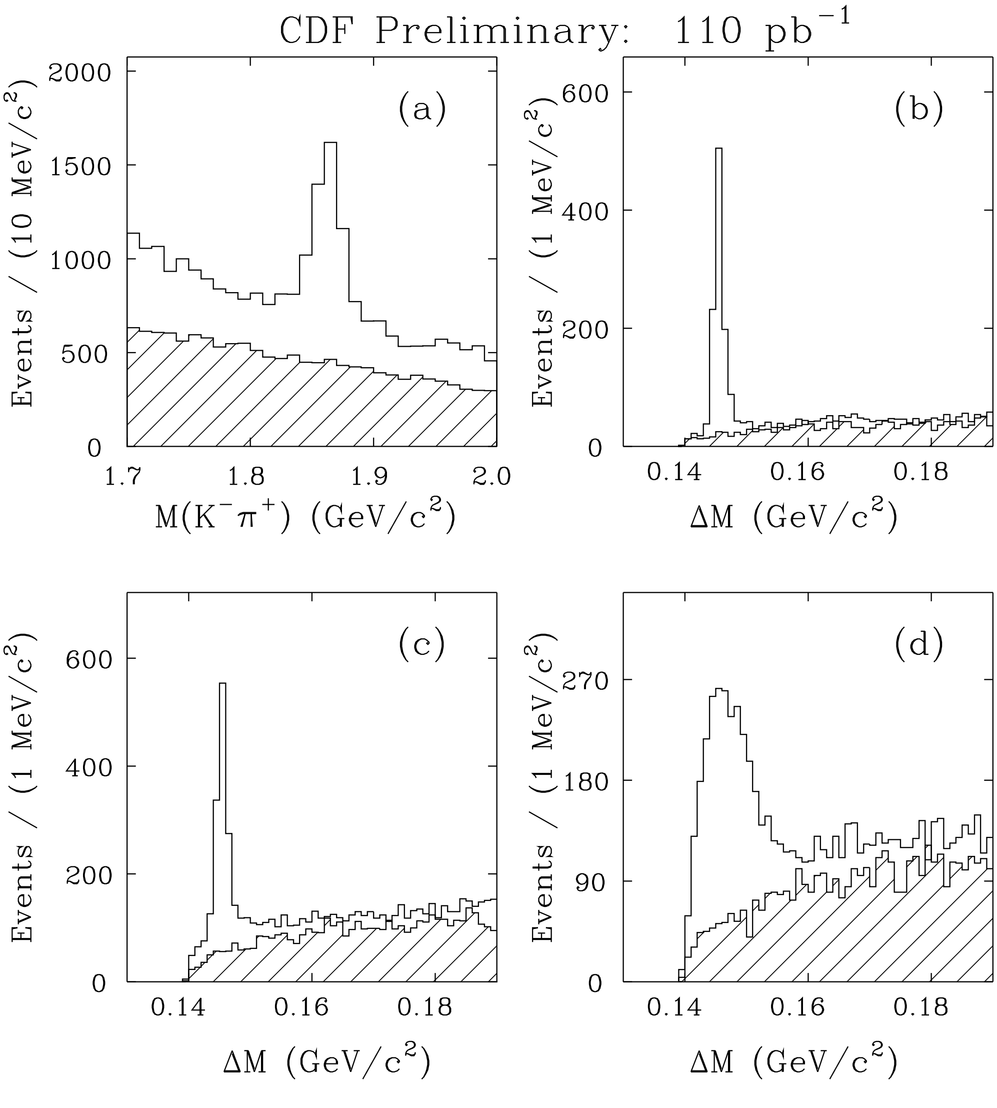

Figure 2.59: Charm signals reconstructed in association with a high-p_T lepton.
(a): Signal for $\bar{B} \to D^0 \ell^- \bar{\nu} X; D^0 \to K^- \pi^+$ (+ c.c.)
(b): Signal for $\bar{B} \to D^{*+} \ell^- \bar{\nu} X; D^{*+} \to D^0 \pi^+; D^0 \to K^- \pi^+$ (+ c.c.)
(c): Signal for $\bar{B} \to D^{*+} \ell^- \bar{\nu} X; D^{*+} \to D^0 \pi^+; D^0 \to K^- \pi^+ \pi^- \pi^+$ (+ c.c.)
(d): Signal for $\bar{B} \to D^{*+} \ell^- \bar{\nu} X; D^{*+} \to D^0 \pi^+; D^0 \to K^- \pi^+ X$ (+ c.c.)
Mode (a) is dominated by B^- decays and modes (b) – (d) by $\bar{B}^0$ decays (ΔM is the mass difference between the $D^0\pi^+$ and the D^0). Shaded histograms show wrong–charge combinations (*e.g.*, $\ell^- K^+$); in (a) these are scaled by 0.5 for display purposes.

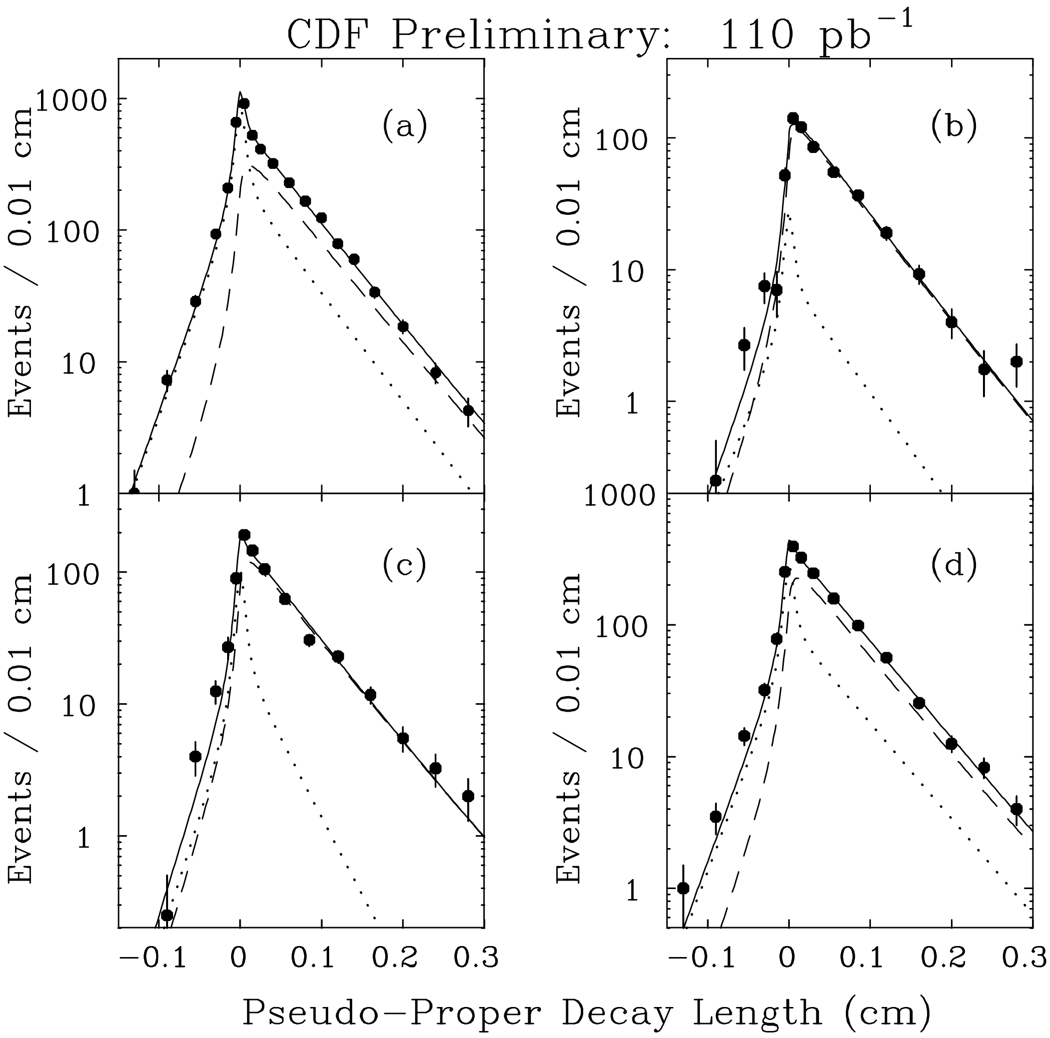

Figure 2.60: Distributions of pseudo-proper decay lengths for lepton + "D" signal samples (points). In all the plots the fits are shown for the signal (dashed line), background (dotted line) and sum (solid line). The four decay channels are represented in (a) – (d) as in the previous figure.

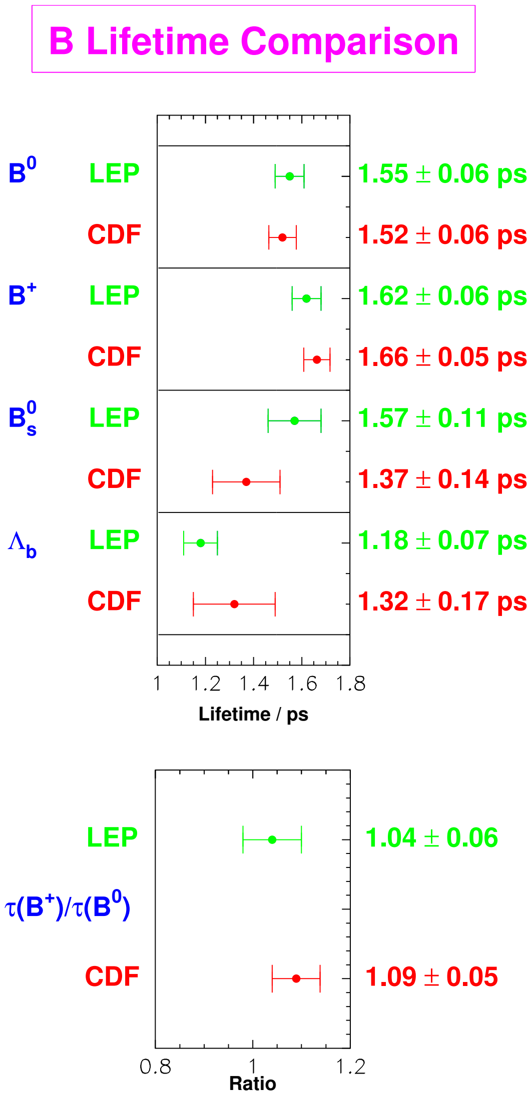

Figure 2.61: CDF and combined LEP (1995) results for b hadron lifetimes.

at low to moderate p_T.

In addition, the high–rate capability of the upgraded trigger/data acquisition system will enable us to handle the high luminosity of the Main Injector era while lowering thresholds and acquiring events in many more channels. Of particular importance will be the ability to form triggers based on track information alone at Level 1 (XFT) and detect the presence of tracks with displaced vertices at Level 2 (SVT).

Thus, the CDF II detector will provide for a competitive b physics program that has unique features and addresses a wide variety of topics of fundamental importance. Below we discuss several specific topics:

- Observation of *CP* violation in $B^0 \to J/\psi K_S$
- Observation of *CP* violation in $B^0 \to \pi^+\pi^-$
- Search for *CP* violation in $B_s \to J/\psi\phi$
- Reconstruction of channels useful for measuring the angle γ.
- Measurement of the ratio of CKM matrix elements $|V_{td}/V_{ts}|$
  - B_s mixing, $\Delta\Gamma_s/\Gamma_s$
  - Radiative B decays
- Observation of the rare decays $B^0 \to \mu\mu K^{*0}$ and $B^\pm \to \mu\mu K^\pm$

These topics are of high priority on our physics menu and they highlight the needed capabilities of the CDF II detector. With these capabilities we also expect to be able to make significant progress on several other topics in b-quark physics, including the observation and study of B_c decays, and on measurements of CKM matrix elements V_{ub} and V_{cb} in exclusive semileptonic decays of B meson and baryons (*e.g.* $B \to \rho\ell\nu$).

2.6.4 *CP* Violation in the B system

2.6.4.1 *CP* Asymmetry in $B^0 \to J/\psi K_S$

By far the most important goal of the CDF II B physics program is the observation of *CP* violation in the B system. The decay mode most frequently discussed in the literature [12] is $B^0 \to J/\psi K_S$. *CP* violation would manifest itself as an asymmetry in the partial decay rates of B^0 and $\bar{B}^0$ to the same final state, $J/\psi K_S$ (a *CP* eigenstate). This will result in an asymmetry:

$$A_{CP} = (N - \bar{N})/(N + \bar{N}) \qquad (2.5)$$

in the number of decays from B^0 (N) and $\bar{B^0}$ ($\bar{N}$) mesons. The asymmetry in the partial decay rates is directly related to the angle β of the CKM unitary triangle:

$$\Gamma(B^0, \bar{B^0} \to J/\psi K_S) \propto e^{-\Gamma t}[1 \pm \sin(2\beta)\sin(x\Gamma t)] \qquad (2.6)$$

where $x = \Delta m/\Gamma$ is the ratio of the mass difference of the heavy and light B meson states to the total decay rate, also known as the mixing parameter, and t is the decay time. The observed asymmetry A_{CP}^{obs} will be smaller than A_{CP} by a factor known as the "dilution" D; $A_{CP}^{obs} = DA_{CP}$. As discussed below the dilution receives contributions from the time evolution of the B meson under study and from the method used to tag the flavor of the B meson at the time of production.

CDF has already collected the world's largest sample of $B^0 \to J/\psi K_S$ decays: a preliminary analysis of the full data sample accumulated in Run I (110 pb^{-1}) results in 240 of these events, shown in Figure 2.62 with S/N better than 1 : 1. We obtained this sample with a dimuon trigger that required both muons to have transverse momentum (p_T) greater than 2.0 GeV/c. For this analysis, we have not required that the events be in the SVX fiducial region, although we used SVX information if available. Also shown in Figure 2.62 is the same data sample with the additional requirement that SVX track information be available for the J/ψ decay muons, demonstrating an improvement in S/N within the limited acceptance of the SVX. The improved capability and increased coverage obtained with the SVX II should result in a much improved signal to noise; in what follows we have conservatively assumed $S/N = 2:1$.

Our goal for Run II is to improve the trigger efficiency to the point that we reconstruct three to four times as many $B^0 \to J/\psi K_S$ events per pb^{-1}. We expect to achieve this by lowering the p_T threshold to 1.5 GeV/c (made possible in Run II by having a tracking trigger at Level 1), by using $J/\psi \to e^+e^-$ as well as $J/\psi \to \mu^+\mu^-$ decays, and by improving the coverage for lepton identification.

The decrease of the muon threshold alone is expected to double the current $\mu^+\mu^- K_S$ yield (events per pb^{-1}). Including the acceptance gained by the completion of the CMX detector, we then expect $\approx 10,000$ events for 2 fb^{-1} from the dimuon triggers in the central region ($|\eta| < 1$, *i.e.* CMU and/or CMX).

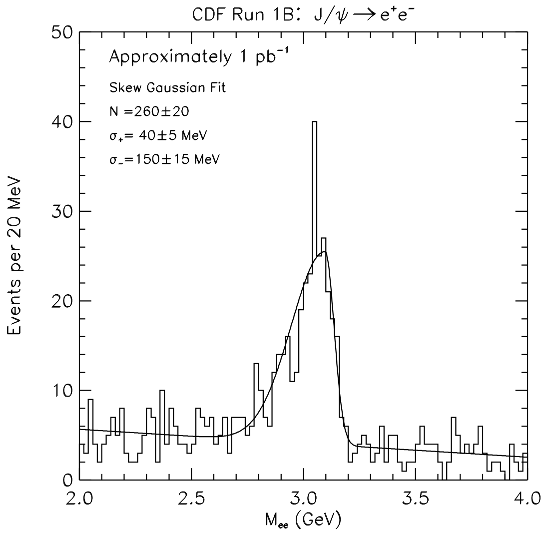

Figure 2.63: $J/\psi \to e^+e^-$ signal from a test trigger during Run I.

The inclusion of electrons was studied with some tests of di–electron triggers during Run I. Figure 2.63 shows a reconstructed $J/\psi \to e^+e^-$ signal obtained with a test trigger based on a 3 GeV/c electron p_T threshold. From these studies it is estimated that a Level 2 trigger rate of 20 Hz could be achieved assuming a 2 GeV/c threshold and the requisite improvements for the CES electronics to cope with the lower threshold and higher crossing frequency for Run II. If possible we wish to use a 1.5 GeV/c threshold; However, in the estimates of sensitivity which follow we assume a 2 GeV/c threshold for electrons, for an overall factor of three increase on the Run I $B^0 \to$ dilepton $+K_S$ yield.

There are also possibilities for further increasing the number of reconstructed $B^0 \to J/\psi K_S$ events, such as improving the coverage for lepton identification beyond the central region. Some of them are listed at the end of this section.

In what follows we will not take any such possible improvements into account, but we investigate only two scenarios, one in which we have only the dimuon channel available for J/ψ reconstruction (resulting in 10,000 $B^0 \to J/\psi K_S$ events) and one in which the

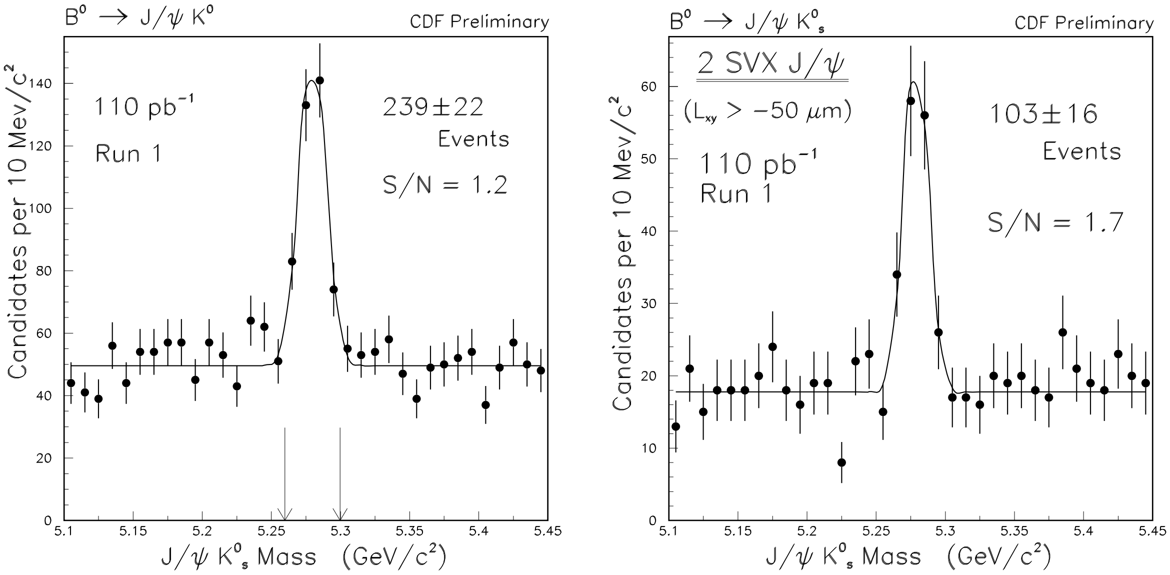

Figure 2.62: CDF's $B^0 \to J/\psi K_S$ signal from Run I. For the plot on the right, SVX track information has been required for muons from the J/ψ. It is noted that the S/N improves to 2.3 : 1 without additional loss of signal if the transverse decay length (L_{xy}) is required to be greater than zero.

di–electron channel is also available, resulting in the total of 15,000 events.

To obtain the CP asymmetry we must tag the flavor of the B meson at the time at which it was produced. The flavor tagging efficiency is more uncertain than the $B^0 \to J/\psi K_S$ yield. We are currently investigating several flavor tagging methods. Work is under way to use a combination of Run I data and Monte Carlo to establish the "effective tagging efficiency" for each possible method with the CDF II detector configuration. The "effective tagging efficiency" is is defined to be ϵD^2 for a flavor tagging method with efficiency ϵ and dilution D. The uncertainty on the CP asymmetry, δA_{CP}, is given by

$$(\delta A_{CP})^2 \approx \frac{1}{\epsilon D^2 N}\frac{S+B}{S} \tag{2.7}$$

where N is the total number of events prior to flavor tagging and $N = S+B$ includes signal (S) and background (B) events (and we assume $S/B = 2:1$). The dilution is defined as $D = (N_R - N_W)/(N_R + N_W)$, where N_R and N_W are the number of events with right and wrong tags respectively.

We currently have results for three flavor tagging methods (the effectiveness of these methods has been demonstrated in our measurements of $B^0 - \bar{B}^0$ mixing as shown later):

1. Jet Charge [13], where the weighted sum of the charge of tracks recoiling against a B meson is used to determine the flavor of the second b hadron in the event

2. Lepton tagging [14], where a lepton from the second b hadron in the event is used to tag its flavor

3. Same-Side Tagging [15], where charge correlations between the B meson and charged tracks in its vicinity are used to identify the flavor of the B meson at the time of production [16].

The sum of the individual ϵD^2 for these three algorithms is $\approx 3.4\%$, although correlations among the flavor tagging methods are expected to reduce the combined effective tagging efficiency. The study of these correlations is in progress. A conservative estimate is that using the three algorithms together results in a combined ϵD^2 which is $\approx 80\%$ of the sum of the individual ϵD^2 for each algorithm.

Table 2.12 lists the tagging methods we expect to exploit, the effective tagging efficiency measured in

Run I, and the elements of the CDF II detector upgrade that impact these algorithms. The dilution effects due to mixing and mistags for the opposite–side tagging algorithms are included in the values given for ϵD^2.

For Run II, we expect improvements in the total ϵD^2 from the following sources:

- An improvement is expected for lepton tagging by extending the coverage beyond the central region, giving a total $\epsilon D^2 = 1.7\%$ from lepton tagging.

- The increased coverage of the SVX II, together with its three-dimensional track reconstruction capability, will result in a cleaner selection of fragmentation tracks around the B meson. We expect ϵD^2 for Same Side Tagging to increase to 2%.

- A significant improvement in ϵD^2 is possible for the Jet Charge algorithm. The extended coverage of the SVX II and ISL and their added pattern recognition capability will enhance substantially the purity of this algorithm. Monte Carlo studies indicate that $\epsilon D^2 \approx 3\%$ is possible.

- Further improvement in ϵD^2 is expected if a Time–of–Flight system is eventually installed. In the current baseline detector design a TOF system is not included; however, there are provisions (*i.e.* empty space) for the installation of such a system at some point in the future. The main motivation for such an addition is the added tagging efficiency ($\epsilon D^2 \approx 3\%$) from using the charge of kaons opposite to the $B^0 \to J/\psi K_S$ decay.

The uncertainty expected on the measurement of $\sin(2\beta)$ is given by

$$\delta \sin(2\beta) \approx \frac{1+x_d^2}{x_d} \frac{1}{\sqrt{\epsilon D^2 N}} \sqrt{\frac{S+B}{S}} \tag{2.8}$$

where $x_d/(1+x_d^2) = 0.47$ accounts for the dilution due to the time evolution of the signal B^0 in a time–integrated asymmetry measurement (for the time being we ignore the improvement afforded by fitting the time development of the asymmetry). The Run II expectation based on the above yields and effective tagging efficiencies is listed in Table 2.13. The effective tagging efficiency includes the 80% derating for overlaps among the flavor tagging algorithms employed.

We consider the estimate of $\delta \sin(2\beta) = 0.13$ to be a very conservative scenario which is essentially established based on Run I data. In the optimistic scenario with the inclusion of dielectron triggers, improved Jet Charge flavor tagging and a TOF system, we could obtain a total $\epsilon D^2 = 7.8\%$ yielding $\delta \sin(2\beta) = 0.076$.

Finally, in addition to the above expectation of $15,000$ $B^0 \to J/\psi K_S$ events in 2 fb^{-1}, the $B^0 \to J/\psi K_S$ yield can be increased by employing (a) the increased tracking coverage and (b) new ways of triggering using the SVT upgrade:

(a) The additional coverage of the IMU for the dimuon trigger can increase the event yield by about 30%. The acceptance for K_S decays is also expected to increase by using tracks at higher pseudorapidity from the ISL.

(b) Simulations of the SVT indicate that it may be possible to trigger requiring one lepton and one additional track with large impact parameter [17]. In the offline analysis, the second lepton is found primarily using tracking information.

In summary, based on the results we have obtained so far, we expect that the dimuon channel, with the improved trigger and coverage, combined with the tagging methods established already, will yield $\delta \sin(2\beta) = 0.13$. Standard Model predictions for $\sin(2\beta)$ are $\sin(2\beta) > 0.17$ [18] and $\sin(2\beta) = 0.65 \pm 0.12$ [19]. Thus, even in the most conservative case, with $\delta \sin(2\beta) = 0.13$, we will have a very interesting measurement of $\sin(2\beta)$ that will probably result in the observation of *CP* violation.

It is likely that we will do better than the conservative case. The addition of the di–electron channel, improved detector performance for Jet Charge flavor tagging and a TOF system would increase the accuracy to $\delta \sin(2\beta) = 0.076$. This level of sensitivity is similar to that which might be achieved after two years of running at 10^{33} cm^{-2}sec^{-1} at the B factories by (appropriately) summing over several final states. As we gain experience, additional triggering and reconstruction techniques may allow an even more precise measurement that will tightly constrain the parameters of the Standard Model.

Tagging Method	ϵD^2 (%) (measured)	ϵD^2 (%) (expected)	Relevant CDF II Upgrade
Central Muon	0.6 ± 0.1	1.0	Complete CMX/Add IMU
Electron	0.3 ± 0.1	0.7	Plug calorimeter/ISL
Same-side pion	1.5 ± 0.4	2.0	SVX II/ISL
Jet Charge	1.0 ± 0.3	3.0	SVX II/ISL
Opposite-side Kaon		3.0	Time–of–Flight

Table 2.12: Flavor tagging methods currently under consideration, the effective tagging efficiency, ϵD^2, for algorithms established with Run I data, the expected ϵD^2 in Run II, and the list of detector upgrades that will improve ϵD^2.

Scenario	ϵD^2 (%)	$N(J/\psi K_S)$	$\delta \sin(2\beta)$
$\mu^+\mu^-$ triggers; "measured" tags only	2.7	10,000	0.16
Improved lepton and same–side π tags	3.8	10,000	0.13
Add $J/\psi \to e^+e^-$ triggers	3.8	15,000	0.11
Improved Jet Charge tag	5.4	15,000	0.09
Add Time–of–Flight	7.8	15,000	0.076

Table 2.13: The expected uncertainty on the measurement of $\sin(2\beta)$ under different assumptions on the total effective tagging efficiency and the number of $J/\psi K_S$ events.

2.6.4.2 *CP* Asymmetry in $B^0 \to \pi^+\pi^-$

A measurement of $\sin(2\alpha)$ in conjunction with $\sin(2\beta)$ provides powerful constraints on the unitarity triangle [20]. The greatest challenge in this measurement is the trigger requirement at a luminosity of $1 \times 10^{32}\mathrm{cm}^{-2}\mathrm{sec}^{-1}$. Our plan (described in detail in Reference [21]) consists of

Level 1: Requiring that two oppositely–charged tracks be found with the XFT track processor (capable of finding tracks in the COT with $p_T >$ 1.5 GeV/c with $\delta p_T/p_T^2 < 0.01$ [GeV/c]$^{-1}$). Imposing $\Delta\phi$ cuts on oppositely–charged 2 GeV/c track pairs yields an expected Level 1 accept rate of 16 kHz as measured using Run I data.

Level 2: Using the SVT processor (capable of extrapolating the XFT tracks in the SVX II detector and determining their impact parameter, d, with resolution $\sigma_d \approx 25\mu$m). Demanding $d > 100$ μm yields an expected Level 2 accept rate of less than 20 Hz.

Level 3: Here the full event information is available. We expect to be able to reduce the rate out of Level 3 to about 1 Hz.

With these trigger requirements we expect ≈ 5 $B^0 \to \pi^+\pi^-$ events per pb^{-1} for a yield of 10,000 events in 2 fb^{-1}. Since these events must pass the SVT requirement, they have a proper lifetime distribution starting at ≈ 1.5 lifetimes. After fitting the time development, the dilution of the *CP* asymmetry due to the time evolution of the signal B will be 0.82, rather than the time averaged value, 0.47, which we assumed for $\sin(2\beta)$.

To measure the *CP* asymmetry in $B^0 \to \pi^+\pi^-$ events one needs to extract the *physics* backgrounds from $B^0 \to K\pi$, $B_s \to K\pi$ and $B_s \to KK$ decays. Figure 2.64 displays the expected mass distribution for the combination of the above four signals, assuming [21] all charged kaons to be pions, equal partial rates for the four decay modes and a 3 : 1 production ratio for $B^0 : B_s$. The $B^0 \to \pi\pi$ and $B^0 \to K\pi$ peaks are separated by 40 MeV/c^2. An initial simulation of the upgraded detector indicates that the resolution at $p_T(B) \approx 6$ GeV/c will be about 20 MeV/c^2. Note that the $B_s \to KK$ peak lies directly under the $B^0 \to \pi\pi$ peak and is not resolved by improved mass resolution and thus particle ID will be required.

In order to extract the $\pi\pi$ signal it will be essential to make use of the dE/dx information provided by the COT. With the CTC we achieve a one standard

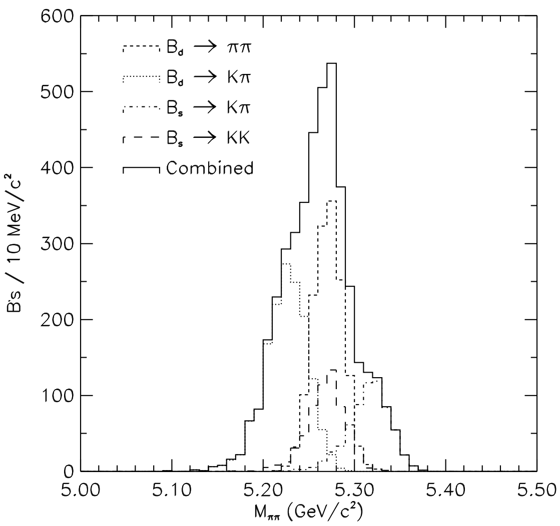

Figure 2.64: Mass distribution for the combination $B^0 \to \pi^+\pi^-$, $B^0 \to K\pi$, $B_s \to K\pi$ and $B_s \to KK$ assuming all charged kaons to be pions. The assumed mass resolution is ~20 MeV/c^2. (Note that the vertical scale should be treated as arbitrary.)

deviation separation between the K and π signals for momenta $>$ 2 GeV/c. We expect the COT dE/dx performance to be as good as that for the CTC and perhaps better due to the increased number of samples and efficiency for dE/dx hit usage. With dE/dx information and the mass distribution we can statistically extract the $B^0 \to \pi\pi$ component from the total invariant mass distribution. It is useful to point out that this evaluation will be carried out with the full sample, that is, before B flavor tagging.

Another issue for this analysis is the combinatorial background under the B peak. Although in the Run I data we expect only a fraction of a signal event, we can estimate the background level for the CDF II detector using inclusive electron data. Using standard cuts on the decay vertex and the isolation of the two-track combination, we obtain an observed background N comparable to the expected signal S for $p_T > 4$ GeV/c on each track: $S/N \approx 1:1$. Lowering the p_T threshold to 2 GeV/c will allow us to double our efficiency. We expect to do this with the CDF II detector while maintaining S/N better than $1:1$ by exploiting the 3D information from the SVX II and optimizing cuts.

The final issue related to the extraction of the angle α from the measured CP asymmetry in $B^0 \to \pi\pi$ is the extraction of possible penguin contributions in addition to the tree diagram which is expected to dominate this decay mode. We can estimate this penguin contamination, and thus extract α, from a combination of experimental measurements and theoretical inputs. A detailed analysis can be found in reference [22]. Assuming a flavor-tagging efficiency (ϵD^2) of 7.8% as in the $J/\psi K_S$ case, and a conservative $S/N = 1/4$, we expect an overall uncertainty on $\sin(2\alpha)$ of 0.10.

2.6.4.3 *CP* Asymmetry in $B_s \to J/\psi\phi$

While the CP asymmetry in $B^0 \to J/\psi K_S$ measures the weak phase of the CKM matrix element V_{td}, the CP asymmetry in $B_s \to J/\psi\phi$ measures the weak phase of the CKM matrix element V_{ts}. The latter asymmetry is expected to be very small in the Standard Model, but in the context of testing the Standard Model has the same fundamental importance as measuring the more familiar CP asymmetries. This measurement is most accessible, if not unique, to experiments at a hadron collider.

Our Run I B_s mass analysis indicates that our yield of reconstructed $B_s \to J/\psi\phi$ events is 60% that of $B^0 \to J/\psi K_S$ (see Figure 2.65). Since the modest trigger improvements for $B^0 \to J/\psi K_S$ ($\approx 15,000$ events) apply equally to $B_s \to J/\psi\phi$, we can expect ≈ 9000 events for this decay mode in Run II.

The flavor tagging techniques described for the B^0 case apply to the B_s with one exception: The fragmentation track correlated with the B_s meson is a kaon instead of a pion. A PYTHIA study indicates that a Time–of–Flight system, by identifying kaons, would allow us to increase the efficiency of the same-side kaon algorithm from 2% to 5% [23]. In this case we could assume a total flavor tagging efficiency (ϵD^2) for B_s mesons of $\approx 10\%$.

The magnitude of a CP asymmetry in $B_s \to J/\psi\phi$ decays will be modulated by the frequency of B_s oscillations. Thus, for a meaningful limit, we must be able to resolve B_s oscillations. If we neglect ($c\tau$) resolution effects, we can expect a precision on the asymmetry of ± 0.09 from a time dependent measurement. However, resolution effects smear the oscillations and produce an additional dilution. For our Run I data, if we determine the primary vertex event-by-event, the proper lifetime resolution for fully reconstructed B decays is $\approx 30\mu$m [24]. We expect that the proper lifetime resolution for the SVX II will be $\approx 10\%$ bet-

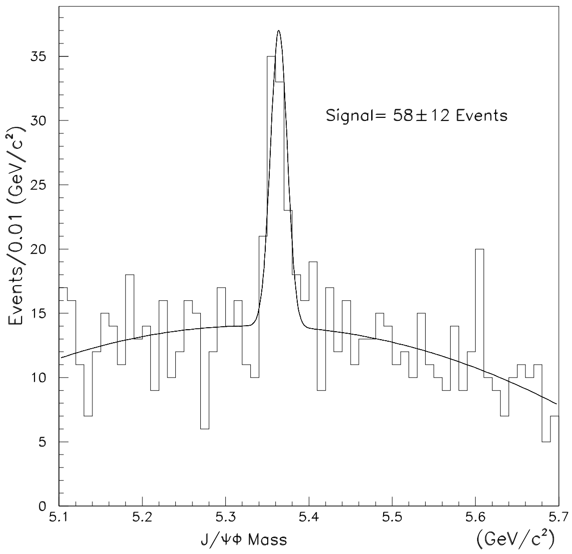

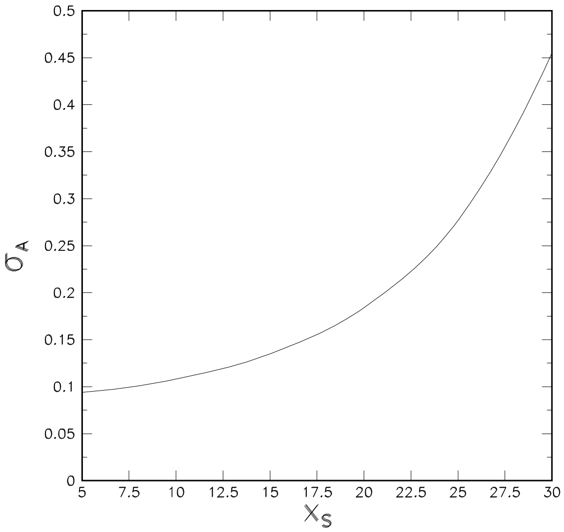

Figure 2.65: Left: The reconstructed mass distribution for $B_s \to J/\psi\phi$ decays. SVX track information has been required for the muons from the J/ψ. Right: The uncertainty on the *CP* asymmetry for $B_s \to J/\psi\phi$ as a function of the B_s mixing parameter x_s.

ter than that for the Run I detector [25]. Figure 2.65 shows our expected precision on the asymmetry as a function of x_s.

2.6.4.4 Feasibility of measuring γ

Measuring the third angle, γ, in the unitarity triangle completes the test of the unitarity of the CKM matrix. The angle γ can be probed via the decays [26]

1. $B_s^0 \to D_s^- K^+$ and $D_s^+ K^-$
2. $B^+ \to \bar{D}^0 K^+$, $B^+ \to D^0 K^+$, and $B^+ \to D^0_{CP+} K^+$

where D_{CP+} refers to the *CP* even state $(|D^0\rangle + |\bar{D}^0\rangle)/\sqrt{2}$.

These decay modes have been considered in Reference [27]. As with the $B^0 \to \pi^+\pi^-$ decay mode, these analyses depend on an all–hadronic decay mode trigger (*i.e.* charged tracks). Assuming a Level 1 trigger of two tracks with opposite charge and $p_T > 2$ GeV/c, and a Level 2 trigger cut of 100 μm on the impact parameter, we expect an overall efficiency times acceptance of $\approx 3 \times 10^{-4}$ for the B_s and $B^\pm$ decay modes above.

Unfortunately, the decay modes $B_s^0 \to D_s^- K^+$ and $D_s^+ K^-$ require a time-dependent analysis and therefore their utility depends on the B_s mixing parameter, x_s. Moreover, the results in Reference [27] indicate that a very small tagged signal is expected. However, if $\Delta\Gamma/\Gamma$ for the B_s is large enough and can be measured independently, γ can be extracted by measuring the relative fraction of the two lifetime components in the untagged $D_s K$ sample. [28] Also, it has been recently noted [29] that a determination of the CKM angle γ may be obtained through measurements of the time evolution of angular distributions for B_s decays into final states which are *CP* admixtures.

The charged B modes are very interesting since the observation of an asymmetry between B^+ and B^- would indicate the presence of direct *CP* violation. Experimentally, measurement of the asymmetry involves only time–integrated quantities; these decays are self–tagging. The uncertainty on the observed *CP* asymmetry is now a function of (a) the angle γ and (b) the strong phase difference, δ. In the most favorable case, $\gamma = \pi/2$ and $\delta = \pi/2$. Then the *CP* asymmetry, A_{CP}, and the uncertainty on it, δA_{CP}, are $A_{CP} = 0.2$ and $\delta A_{CP} = 0.05$ respectively. The detailed discussion of the uncertainty on A_{CP} is contained in [27].

2.6.5 Determination of $|V_{td}/V_{ts}|$

Within the CKM model, $|V_{td}/V_{ts}|$ is constrained at 95% confidence level to lie in the range [18]:

$$0.11 \leq \left|\frac{V_{td}}{V_{ts}}\right| \leq 0.36 \tag{2.9}$$

Experiments operating on the $\Upsilon(4S)$ can determine $|V_{td}/V_{ts}|$ by measuring the ratio of decay rates of radiative B decays $B(B \to \rho\gamma)/B(B \to K^*\gamma)$ [30]. However, recent studies [31] have shown that such decays have potentially large long-distance contributions, making extraction of $|\frac{V_{td}}{V_{ts}}|$ difficult.

In contrast, experiments at hadron colliders can also use B_s mesons, which are amply produced, and determine $|V_{td}/V_{ts}|$ using several independent techniques, including some with quite small theoretical uncertainties as discussed below. Combining these techniques, CDF II should, with 2 fb^{-1} of data, not only be able to constrain $|V_{td}/V_{ts}|$, but also *measure* its value over the full range permitted by the Standard Model.

2.6.5.1 B_s Mixing

Mixing in the B system has been discussed extensively in the literature [18]. In the Standard Model, $B\overline{B}$ oscillations occur dominantly through top quark contributions to the electroweak box diagram. The size of the mixing is expressed in terms of the parameter $x \equiv \Delta m/\Gamma$ where Δm is the difference in mass between the heavy and light B meson states and $\Gamma = \hbar/\tau$ where τ is the average lifetime of the states. The value of x depends on the top quark mass, the B decay constant, the QCD bag parameter and corrections due to the breaking of SU(3) flavor symmetry. Theoretical uncertainties in the determination of the CKM parameters can be greatly reduced by considering the ratio of x_s to x_d:

$$\frac{x_s}{x_d} = \frac{(m_{B_s}\eta_{B_s}B_{B_s}f^2_{B_s})}{(m_{B_d}\eta_{B_d}B_{B_d}f^2_{B_d})}\left|\frac{V_{ts}}{V_{td}}\right|^2 \tag{2.10}$$

where η_{B_i} are QCD corrections of order 1 ($i = d, s$), B_{B_i} are B meson bag parameters, and f_{B_i} are B meson weak decay constants.

In the limit of SU(3) symmetry, the factors in front of the ratio of CKM elements would be unity. Lattice Gauge theory determines the value of these factors to be 1.3 ± 0.2 [32]. Since x_d/x_s depends on $|\frac{V_{td}}{V_{ts}}|^2$, the theoretical uncertainty on $|V_{td}/V_{ts}|$ is $\sim 10\%$.

Because x_s is large, it must be determined by fitting the time-dependent oscillation

$$\text{Prob}(B_s \to \overline{B}_s) = \frac{1}{2}e^{-t/\tau}\left(1 - \cos(x_s t/\tau)\right). \tag{2.11}$$

The quality of the measurement depends upon the experimental proper decay time resolution and the ability to tag the flavor of the B at production time. CDF has already performed measurements of x_d (see Figures 2.66 and 2.67) [33]. Because B_s oscillations are rapid, an x_s measurement will place stringent demands on the experiment's ability to determine the proper time of the decay.

Vertex finding requirements for the x_s measurement are discussed in detail in Reference [34]. In general, the proper time resolution can be parameterized in terms of two constants

$$\sigma_t = \sqrt{a^2 + b^2t^2} \tag{2.12}$$

Here a is determined from the resolution on the primary and secondary vertex positions and b depends on the accuracy with which the momentum of the B_s is known. The decay time t and its uncertainty σ_t are measured in units of proper time, relative to the B_s lifetime. The values of a and b depend upon the decay mode under consideration. In general, the resolution is significantly worse for semileptonic decays ($B_s \to D_s\ell\nu$) than for fully–reconstructed events ($B_s \to D_s + \text{n}\pi$). The number of semileptonic decays is, however, significantly larger. The x_s reach of both decay modes has been studied [35].

CDF already has experience analysing semileptonic B_s decays. In the Run I data [36], 254 ± 21 $B_s \to D_s\ell\nu$ events were reconstructed and a B_s lifetime measurement of $1.37 \pm 0.13 \pm 0.04$ ps was obtained (see Figure 2.68). For Run II, triggering and reconstruction of this channel with very high statistics is straightforward. Our x_s reach will be limited by our proper lifetime resolution. Simulation studies of the SVX II detector [25] have determined that for semileptonic decays $a = 0.11$ and $b = 0.15$. This resolution limits the measurement to values of x_s less than about 15.

For fully–reconstructed decays $a = 0.06$ and $b = 0.03$ [37]. This value of a is based on our Run I proper lifetime resolution using fully reconstructed B events for which we determine the primary vertex event by event. Figure 2.69 shows that with sufficient statistics (the figure contains 2000 fully reconstructed events with perfect tagging) oscillations can

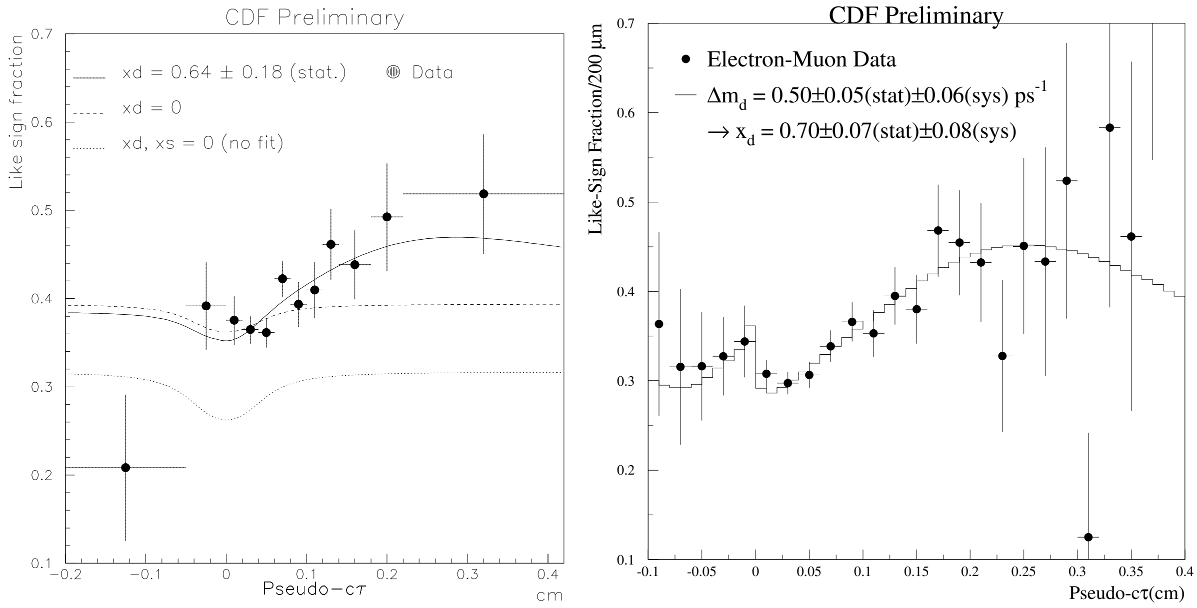

Figure 2.66: Two studies of $B^0 - \bar{B}^0$ mixing performed by CDF using different dilepton triggers. Results of a fit to the like-sign fraction vs proper lifetime are shown on the left for a Run Ia sample (20 pb^{-1}) collected using a dimuon trigger and on the right for a combined Run Ia and Run Ib sample (110 pb^{-1}) collected with an electron-muon trigger. In both cases, one lepton was associated with a secondary vertex and the other lepton served as a flavor tag. For these fits, maximal B_s mixing is assumed.

still be clearly resolved in the SVX II for $x_s = 20$. In practice, the ultimate x_s reach for fully reconstructed decays will depend on the number of decays available in the channel rather than on the proper lifetime resolution. The challenge for CDF II is to trigger on, and isolate from background, signals of this type.

One trigger strategy is to trigger on a single lepton (e or μ), which will serve as the flavor tag, and then reconstruct B_s decays in this sample [34]. For a 6 GeV lepton threshold in Run II, and using selection criteria similar to those commonly used in Run I analyses, the expected yield is low, $\sim$ 250 events. However, it is likely that the lepton trigger threshold could be lower with some of the decay products of the B_s included in the trigger requirement as well. We note that the presence of a Time–of–Flight system in CDF II could significantly improve the reconstruction purity by allowing efficient selection of kaons and rejection of pions at low P_T, where the backgrounds are largest.

A promising strategy is to use a fully hadronic trigger, in which case all tagging techniques may be applied. In fact, the Level 1 and Level 2 triggers designed for $B \to \pi^+\pi^-$ will also provide good acceptance for the decay products of the B_s. Using the same assumptions as for $B_d \to \pi^+\pi^-$, we expect a yield of more than 1600 fully reconstructed and tagged B_s decays. We show in Figure 2.69 the resulting precision on x_s as a function of x_s.

2.6.5.2 $\Delta\Gamma_s/\Gamma_s$

The calculation of x_s depends upon the evaluation of the real part of the mass matrix element. The imaginary part of the same matrix describes the decay widths of the two mass eigenstates B_s^H and B_s^L. Within the Standard Model it is possible to calculate the ratio $\Delta\Gamma_{B_s}/\Delta m_{B_s}$ [38]:

$$\Delta\Gamma_{B_s}/\Delta m_{B_s} = -\frac{3}{2}\pi\frac{m_b^2}{m_t^2}\frac{\eta_{QCD}^{\Delta\Gamma_{B_s}}}{\eta_{QCD}^{\Delta m_{B_s}}} \tag{2.13}$$

where the ratio of the QCD correction factors (η) in the numerator and denominator is expected to be of order unity [39]. This ratio does not depend on CKM parameters. Thus, a measurement of $\Delta\Gamma_{B_s}$ determines Δm_{B_s} up to QCD uncertainties. Moreover, the larger Δm_{B_s} becomes the larger $\Delta\Gamma_{B_s}$ is. Thus,

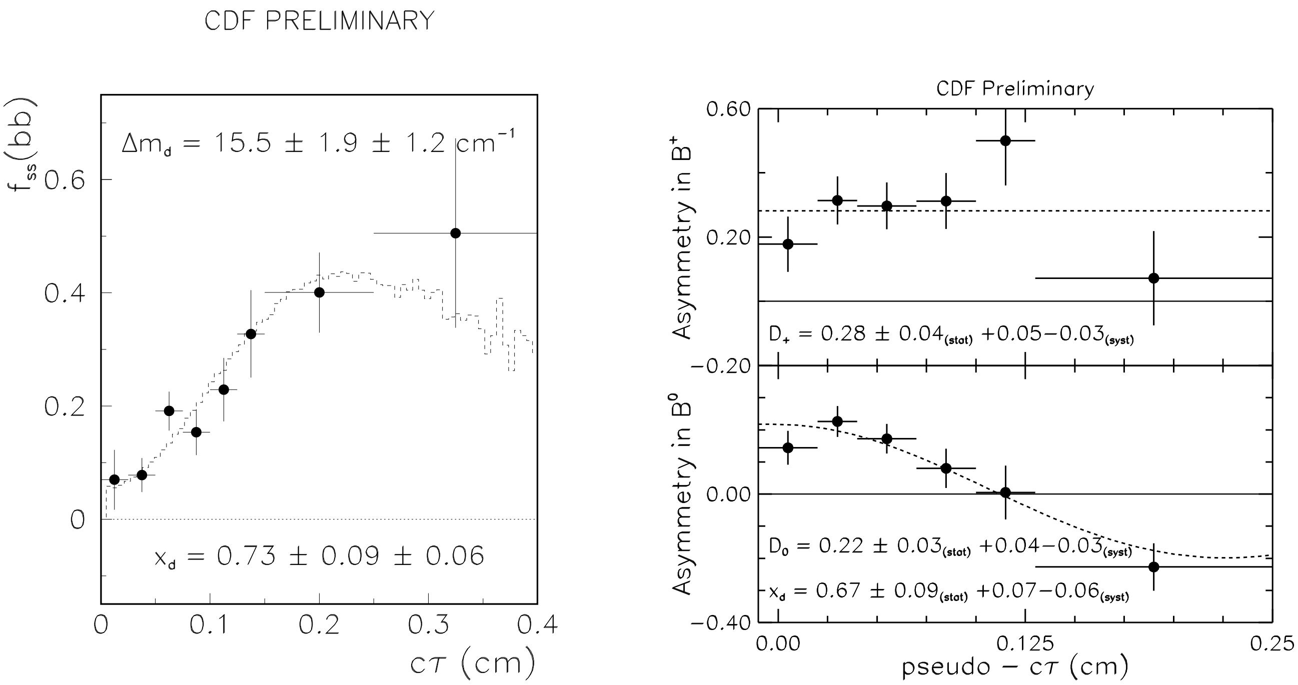

Figure 2.67: Two studies of $B^0 - \bar{B}^0$ mixing performed by CDF using lepton triggers and different tagging strategies. Left: The $b\bar{b}$ same sign fraction as a function of proper time for events from the Run Ib inclusive electron and muon triggers. The trigger lepton is associated with a secondary vertex which gives the proper time. An additional soft lepton or the jet charge of an opposite side jet is used for a flavor tag. The dashed histogram represents the result of an unbinned likelihood fit for Δm_d. Right: Measurement of the asymmetry $(N_R - N_W)/(N_R + N_W)$ as a function of proper time for charged B (upper plot) and neutral B (lower plot) mesons reconstructed from a single lepton trigger sample and flavor tagged using a same-side pion tag. Here, the charge of the B meson is determined by reconstructing the D^0 or D^{*+} meson from the semileptonic decay. A clear mixing signal is present for the neutral B while no mixing is observed for charged B mesons.

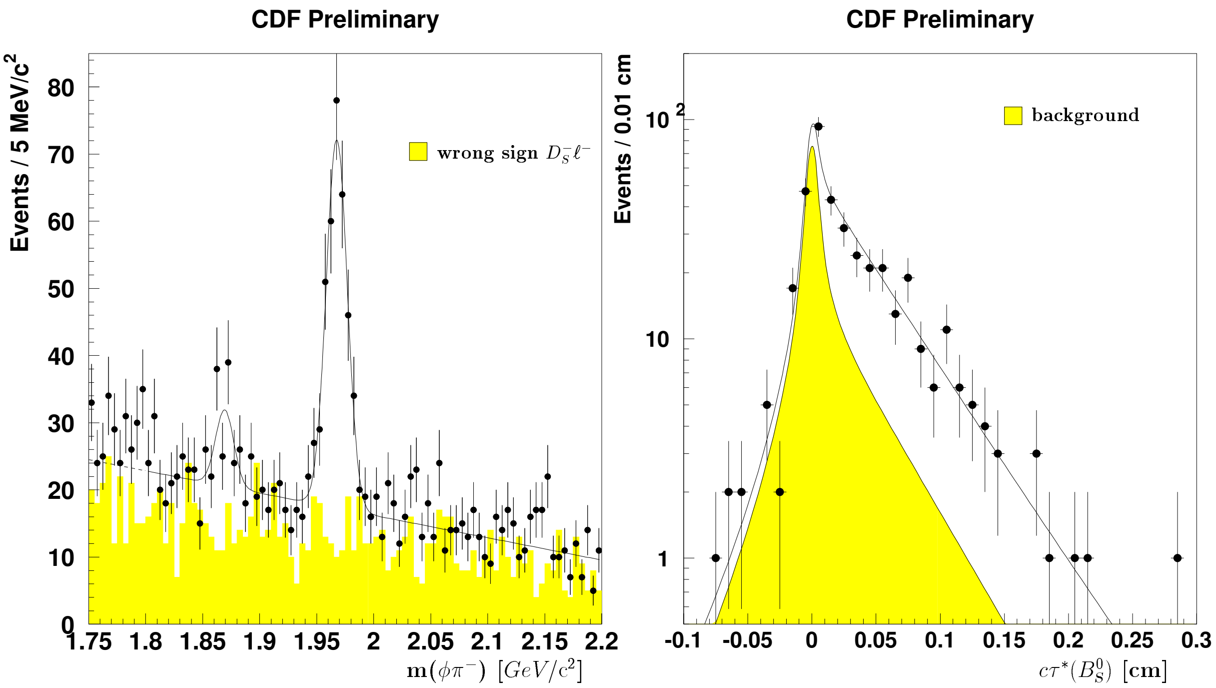

Figure 2.68: Left: invariant mass distribution for D_s mesons produced in right-sign $(D_s^+\ell^-)$ events with $D_s^+ \to \phi\pi^+$ and $\phi \to K^+K^-$; the wrong-sign combinations are shown as a shaded histogram. There is also evidence of the Cabibbo suppressed decay $D^+ \to \phi\pi^+$. Right: pseudo–ctau distributions for the B_s signal and background (shaded).

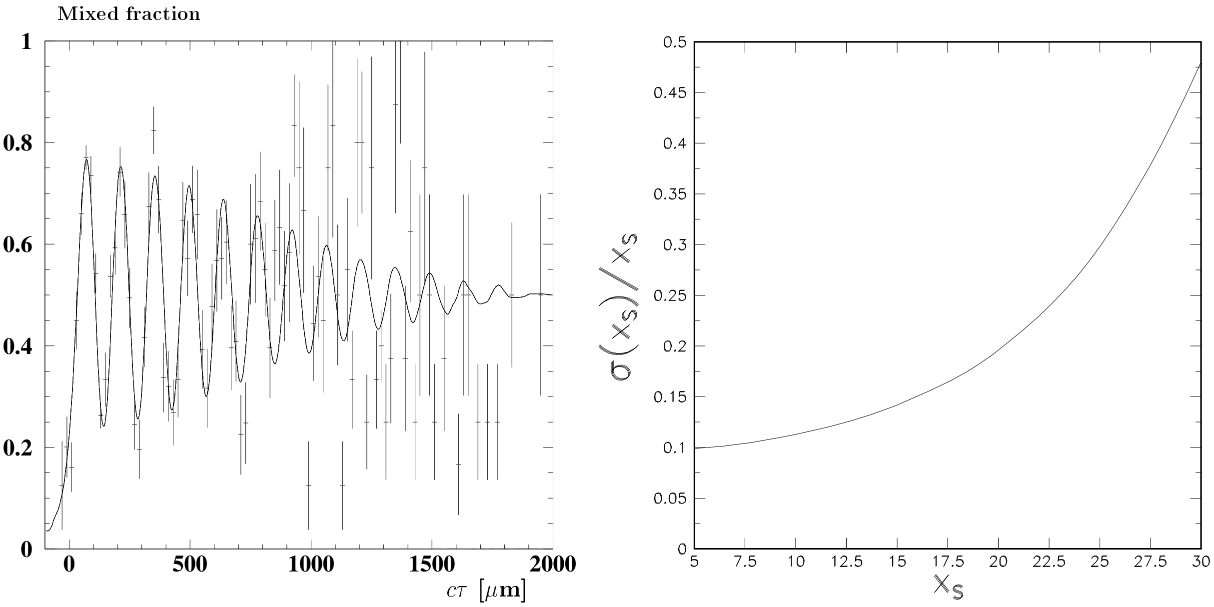

Figure 2.69: Left: A Monte Carlo simulation of the reconstructed B_s mixing signal for a Run II sample with the CDF II detector. Right: Relative uncertainty on x_s for fully reconstructed B_s decays.

as it becomes more difficult to measure x_s, $\Delta\Gamma$ becomes more accessible. Using the above expression, Browder *et al.* [39] show that if $x_s = 15$, a 7% difference in lifetime is expected.[2] They estimate that the uncertainties in calculating $\Delta\Gamma/\Delta m$ contribute an uncertainty of $\sim 30\%$ on $|V_{td}/V_{ts}|^2$ (*i.e.* a 15% uncertainty on $|V_{td}/V_{ts}|$). This contribution to the theoretical uncertainty should be added in quadrature to the 10% uncertainty discussed in the previous section, for a total uncertainty of $\approx 20\%$.

Several techniques can be used to determine $\Delta\Gamma_{B_s}$ [40]. First, the proper time distribution of a flavor-specific B_s mode (*e.g.* $B_s \to D_s \ell \nu$) can be fit to the sum of two exponentials. Second, the average lifetime of such a flavor specific mode can be compared to the lifetime of a mode that is dominated by a single *CP* state (it is expected that $B_s \to J/\psi\phi$ will be such a mode) [41]. Finally, a decay such as $B_s \to J/\psi\phi$ can be decomposed into its two *CP* components (via a transversity analysis [42]) and fit for a separate lifetime for each component. It is noted that CDF has measured the helicity structure of the decays $B \to J/\psi K^*$ and $B_s \to J/\psi\phi$ using Run Ia data [7]. The results obtained are $\Gamma_L/\Gamma = 0.65 \pm 0.10 \pm 0.04$ for $B \to J/\psi K^*$ and $\Gamma_L/\Gamma = 0.56 \pm 0.21 \pm 0.03$ for $B_s \to J/\psi\phi$.

The statistical uncertainty on the B_s lifetime from semileptonic B decays in Run II will be below 1%. The Run II expectation, including only the modest set of trigger improvements described in section 2.6.4.1, is for ≈ 9000 $B_s \to J/\psi\phi$ events. The $B_s \to J/\psi\phi$ helicity structure should then be known to about 1% [3]. Using the current CDF number for the $B_s \to J/\psi\phi$ helicity structure, with 2 fb^{-1}, the lifetime difference could be determined to $2-3\%$. Including current theoretical uncertainties of 20%, this determination of $\Delta\Gamma_{B_s}$ would either measure $|V_{td}/V_{ts}|$ or set an *upper* bound on $x_s \leq 15$. Thus, using the direct x_s measurement and $\Delta\Gamma_s/\Gamma_s$, CDF II should be able to measure $|V_{td}/V_{ts}|$ over the full range permitted by the Standard Model in Run II.

It is important to note that the discussion of B_s mixing (and *CP* violation) has been in the context of the three generation Standard Model. New physics

[2]This large $\Delta\Gamma_{B_s}$ is possible because there are large branching fraction common decay modes available to the B_s and $\overline{B_s}$ (*e.g.* $D_s^{(*)+} D_s^{(*)-}$).

[3]The systematic uncertainties in the polarization measurements are dominated by the estimate of the size and helicity of the background under the B mass peak. These systematic uncertainties should scale with the square root of the number of events in the sample.

associated with large mass scales can also reveal itself through a study of the mass and width differences for the neutral B mesons [43].

2.6.5.3 Radiative B Decays

In the absence of long distance effects, radiative B decays provide an alternative approach for measuring $|V_{td}/V_{ts}|$.

$$\frac{B(B^- \to \rho^- \gamma)}{B(B^- \to K^{*-}\gamma)} = \frac{B(B^0 \to \rho^0\gamma) + B(B^0 \to \omega\gamma)}{B(B^0 \to K^{*0}\gamma)} = \left|\frac{V_{td}}{V_{ts}}\right|^2 \xi\Omega$$

where Ω is a phase space correction and ξ is a model dependent factor in the range 0.58 - 0.81 [30]. The relative rates for $\rho^0\gamma$ and $\omega\gamma$ decays are equal in the quark model. Based upon a 2 fb^{-1} sample containing 13 $K^*\gamma$ candidates (with an estimated background of 1.9) and 2 $\rho\gamma + \omega\gamma$ candidates (with an estimated background of 4.1), CLEO has used this technique to set a bound on $|V_{td}/V_{ts}|$ in the range 0.64 - 0.76, depending upon theoretical model [44].

CDF has already installed a trigger to collect radiative penguin decays (see Reference [45] for details). The limited bandwidth available of the Run I trigger and data acquisition system required the trigger to have quite high thresholds (10 GeV photon plus two 2 GeV tracks). The expected yield with this trigger is ≈ 20 γK^* events per 100 pb^{-1}. In Run II, we expect to lower the photon E_t threshold to 5 GeV and the track P_t threshold to 1.5 GeV, with a resulting yield of $\sim$ 135 events per 100 pb^{-1} or $\sim$ 2700 for 2 fb^{-1}.

The mass resolution of the reconstructed B is dominated by the resolution on the photon energy and is $\sim$ 140 MeV. We have studied our ability to reject combinatorial background using Run Ia photon data and have studied with Monte Carlo the discrimination against $B \to K^*\pi^0$ and $\rho\pi^0$ and higher multiplicity penguin decays [45]. These backgrounds are manageable. However, the offline cuts to remove background are expected to reduce the signal by about a factor of 2. The mass resolution is not adequate to separate $\gamma\rho$ from γK^* on an event-by-event basis; however, a statistical separation is possible. In addition, the COT dE/dx system should provide 1σ K-π separation in the momentum range of interest.

These radiative B decays can also be observed using converted photons. The probability for a photon to convert ($\sim$ 5%) will be offset by a lower photon E_t threshold. Also, the mass resolution is $\sim$ 5 times better than for the signals with unconverted photons and the γ/π^0 separation is $\approx$20 times better, allowing a cleaner separation between $B \to \gamma K^*$ and $B \to \gamma\rho$.

At the Tevatron it is possible to study B_s penguin decays as well. Information on $|V_{td}/V_{ts}|$ can be obtained in the same manner as above from studying the ratio of $B(B_s \to \gamma K^*)/B(B_s \to \gamma\phi)$. The size of the B_s penguin sample is expected to be 1/2 to 1/3 the size of the B_d sample. Comparison of the two results would help constrain the size of the long distance contributions to the decays.

2.6.6 B_c and Cabibbo suppressed decays

CDF II will continue to search for and study additional b hadron states. Figure 2.70 shows the CDF limit on B_c production and decay to $J/\psi\pi$. The study of this $q\bar{q}$ system would be particularly interesting because of the unequal heavy quark masses [46].

We also note that the decay $B^+ \to J/\psi\pi^+$ is a Cabibbo and color suppressed decay which may exhibit a *direct CP* violating effect at the few percent level [47]. The mode is self–tagging and no time dependence is required. Any non–vanishing effect would immediately exclude the superweak model of *CP* violation. In Run II, extrapolating from the ≈ 30 events observed, we expect about a 3% error on the asymmetry.

2.6.7 Rare B decays

Rare B decays provide a stringent test of the Standard Model for possible new physics effects, such as an anomalous magnetic moment of the W and the presence of a charged Higgs. Experimentally, these rare decays are accessible via the dimuon trigger. Using these triggers, CDF has performed a search for the decay modes $B^\pm \to \mu^+\mu^-K^\pm, B^0 \to \mu^+\mu^-K^{*0}$ and $B_{d,s} \to \mu^+\mu^-$. The Standard Model predictions [48] for the branching ratio for these decay modes, together with the expected sensitivity for CDF II, are listed in Table 2.14. The projections for $B^\pm \to \mu^+\mu^-K^\pm$ and $B^0 \to \mu^+\mu^-K^{*0}$ conservatively assume the same signal-to-noise ($\sim 1:10$) as obtained for the Run Ia searches. We expect that a CDF II analysis will benefit from a much improved signal-to-noise.

Assuming Standard Model branching ratios for $B^+ \to \mu^+\mu^-K^+$ and $B^0 \to \mu^+\mu^-K^{*0}$, we will have

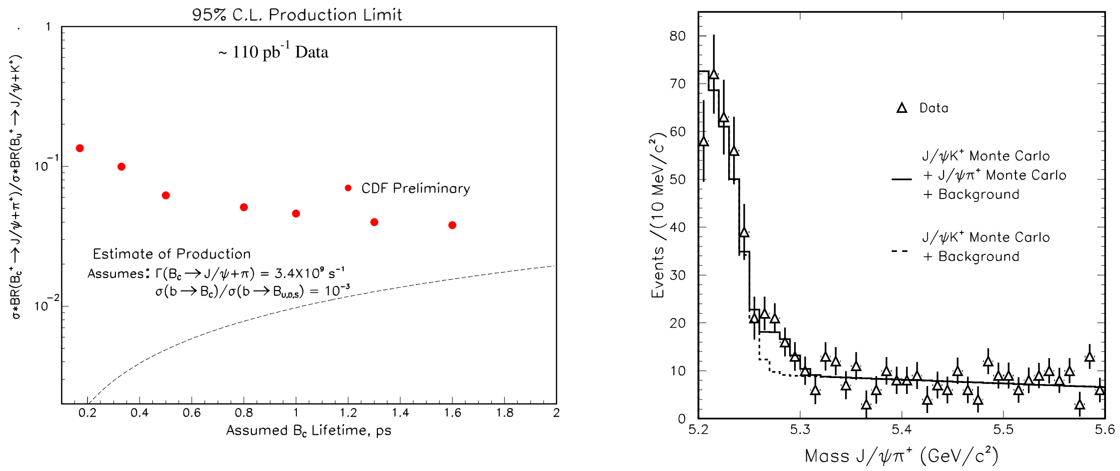

Figure 2.70: On the left: Limit from Run I on the ratio of production and decay of $B_c \to J/\psi\pi$ vs. $B^+ \to J/\psi\pi^+$ as a function of lifetime. On the right: the signal for $B^+ \to J/\psi\pi^+$ is seen as an enhancement in the $J/\psi\pi$ distribution at the upper edge of the $J/\psi K$ contribution which dominates the lower edge of the plot.

B Decay Mode	Standard Model	CDF Run I	CDF II
$\mu^+\mu^-K^+$	$(2-5)\times10^{-7}$	1.0×10^{-5}(20 pb^{-1})	2×10^{-7}
$\mu^+\mu^-K^{*0}$	$(2-5)\times10^{-6}$	2.5×10^{-5}(20 pb^{-1})	4×10^{-7}
$B_d\to\mu^+\mu^-$	$(0.6-1.9)\times10^{-10}$	2.6×10^{-7} (110 pb^{-1})	1×10^{-8}
$B_s\to\mu^+\mu^-$	$(1.5-4.5)\times10^{-9}$	7.7×10^{-7} (110 pb^{-1})	4×10^{-8}

Table 2.14: Rare B decay modes, Standard Model predictions for their branching ratios, 90% limits set with Run I CDF data and the expected sensitivity (90% CL) for CDF II.

visible signals for these decays. In particular, we expect $\approx$ 100 to 300 $B^+ \rightarrow \mu^+\mu^- K^+$ and $\approx$ 400 to 1100 $B^0 \rightarrow \mu^+\mu^- K^{*0}$ events. This will enable us to study both (a) the invariant mass distribution of the dimuon pair and (b) the forward-backward charge asymmetry in the decay. Both of these distributions are sensitive to physics beyond the Standard Model, *e.g.* the presence of a charged Higgs or charginos [49], [50],[51].

2.6.8 Concluding remarks

From the previous discussion it should be clear that CDF II plans to fully exploit the copious production of b hadrons in all of the species produced at the Tevatron. We believe we will have a complete and competitive program, with unique strengths for example in rare decays and B_s physics.

With the experience gained so far in the analyses of Run I data and the planned capabilities of the CDF II detector we are able to confidently project our expectations for Run II which include:

- Observation of *CP* violation in $B^0 \rightarrow J/\psi K^0_S$ and measurement of $\sin(2\beta)$ to better than ± 0.13.
- Observation of *CP* violation in $B^0 \rightarrow \pi^+\pi^-$ and measurement of $\sin(2\alpha)$ to better than ± 0.14.
- Determination of $|V_{td}/V_{ts}|$ with a precision of 20% over the full range allowed by the Standard Model
- Observation of the rare decays $B^0 \rightarrow \mu\mu K^{*0}$ and $B^\pm \rightarrow \mu\mu K^\pm$

With these and other measurements that we will pursue with b hadrons with CDF II, we expect to impose severe constraints on the Standard Model of weak quark mixing and *CP* violation and be very sensitive to new physics.

Bibliography

[1] L. Wolfenstein, Phys. Rev. Lett. **51**, 1945 (1984).

[2] "Measurement of the Mass of the B_s^0 Meson." F. Abe *et al.*, Phys. Rev. **D53** 3496 (1996); "Observation of the Decay $B_s^0 \to J/\psi\phi$ in $p\overline{p}$ Collisions at $\sqrt{s}$ = 1.8 TeV." F. Abe *et al.*, Phys. Rev. Lett. **71** 1685 (1993).

[3] "Observation of $\Lambda_b \to J/\psi\Lambda^0$ at the Fermilab Proton–Antiproton Collider." F. Abe *et al.*, FERMILAB-PUB-96/270-E, August 1996. Submitted to Phys. Rev. D.

[4] "Measurement of the Average Lifetime of B Hadrons Produced in $p\overline{p}$ Collisions at $\sqrt{s}$ = 1.8 TeV." F. Abe *et al.*, Phys. Rev. Lett. **71** 3421 (1993); "Measurement of the B^+ and B^0 Meson Lifetimes." F. Abe *et al.*, Phys. Rev. Lett. **72** 3456 (1994).; "Measurement of the B and $\bar{B}$ Meson Lifetimes Using Semileptonic Decays." F. Abe *et al.*, Phys. Rev. Lett. **76** 4462 (1996).

[5] "Measurement of the B_s^0 Meson Lifetime." F. Abe *et al.*, Phys. Rev. Lett. **74** 4988 (1995); "Measurement of the Lifetime of the B_s^0 Meson Using the Exclusive Decay Mode $B_s^0 \to J/\psi\phi$." F. Abe *et al.*, Phys. Rev. Lett. **77** 1945 (1996).

[6] "Measurement of Λ_b^0 Lifetime Using $\Lambda_b^0 \to \Lambda_c^+\ell^-\bar{\nu}_\ell$." F. Abe *et al.*, Phys. Rev. Lett. **77** 1439 (1996).

[7] "Measurement of the Polarization in the Decays $B_d^0 \to J/\psi K^{*0}(892)$ and $B_s^0 \to J/\psi\phi$." F. Abe *et al.*, Phys. Rev. Lett. **75** 3068 (1995).

[8] "Measurement of the Branching Fraction for $B^+ \to J/\psi\pi^+$ and Search for $B_c^+ \to J/\psi\pi^+$. F. Abe *et al.*, FERMILAB-PUB-96/300-E, September 1996. Submitted to Phys. Rev. Lett.

[9] "Search for Flavor Changing Neutral Current in B Meson Decays in $p\overline{p}$ Collisions at $\sqrt{s}$ = 1.8 TeV." F. Abe *et al.*, Phys. Rev. Lett. **76** 4675 (1996).

[10] "A Measurement of the B Meson and b Quark Cross-Sections at $\sqrt{s}$ =1.8 TeV Using the Exclusive Decay $B^\pm \to J/\psi K^\pm$." F. Abe *et al.*, Phys. Rev. Lett. **68** 3403 (1992); "Measurement of the Bottom Quark Production Cross-Section Using Semileptonic Decay Electrons in $p - \overline{p}$ Collisions at $\sqrt{s}$ = 1.8 TeV". F. Abe *et al.*, Phys. Rev. Lett. **71** 500 1993); "Measurement of Bottom Quark Production in 1.8-TeV $p\overline{p}$ Collisions Using Semileptonic Decay Muons." F. Abe *et al.*, Phys. Rev. Lett. **71** 2396 (1993); "Measurement of the B Meson and b Quark Cross-Sections at $\sqrt{s}$ =1.8-TeV using the Exclusive Decay $B_d^0 \to J/\psi K^{*0}(892)$." F. Abe *et al.*, Phys. Rev. **D50** 4252 (1994). "Measurement of the B Meson Differential Cross-Section, $\frac{d\sigma}{dP_t}$, in $p - \overline{p}$ Collisions at $\sqrt{s}$ = 1.8 TeV." F. Abe *et al.*, Phys. Rev. Lett. **75** 1451 (1995).

[11] "Measurement of Correlated $\mu - \bar{b}$ Jet Cross Sections in $p\overline{p}$ Collisions at $\sqrt{s}$ =1.8 TeV." F. Abe *et al.*, Phys. Rev. **D53** 1051 (1996). "Measurements of $b\bar{b}$ Production Correlations, $B\bar{B}$ Mixing and a Limit on ϵ_B." F. Abe *et al.*, FERMILAB-PUB-96/216-E, August 1996. Submitted to Phys. Rev. D.

[12] H. Quinn, *B^0–$\bar{B}^0$ Mixing and CP Violation in B Decay*, in Review of Particle Properties, Phys. Rev. **D50**, 1632 (1994) and references therein.

[13] O. Long and J. Kroll, *A Jet Charge B-Tagging Method*, CDF note 3069. See also CDF note 3810.

[14] M. D. Peters *et al.*, *A Study of B-Flavor Tagging Using Soft Muons*, CDF note 3098. See also CDF notes 3808 and 3809.

[15] *Observation of $\pi - B$ Charge–Flavor Correlations and Measurement of Time-Dependent $B\bar{B}$ Mixing in $p\overline{p}$ Collisions*, The CDF Collaboration. Contributed paper to the XXVIII Inter-

national Conference on High Energy Physics, Warsaw, 1996, FERMILAB-CONF-96/175-E. K. Kelley and P. Sphicas, *Same-Side Tagging in Exclusive B decays*, CDF note 3638.
F. DeJongh, P. Maksimovic and P. Sphicas, *An Investigation of Time–Dependent B^0 Mixing in Tagged Lepton+Charm Events*, CDF note 3644. See also CDF note 3701.

[16] M. Gronau and J.L. Rosner, Phys. Rev. **D49**, 254 (1994).

[17] S. Belforte *et al.*, *Silicon Vertex Tracker (SVT) Technical Design Report*, CDF note 3108.

[18] A. Ali and D. London, Z. Phys. **C65**, 431 (1995).

[19] M. Ciuchini *et. al.*, Z. Phys. **C68**, 239 (1995).

[20] M.E. Lautenbacher, Proceedings of the 27th Int. Conf. on High Energy Physics, Glasgow, Scotland, 20-27 Jul 1994.

[21] S. Donati and G. Punzi $B^0 \rightarrow \pi^+\pi^-$ *Trigger Studies with Run Ia Data*, CDF note 3167; J. Mueller and P. Wilson, *A 2 Track $B \rightarrow \pi\pi$ Trigger for Run II*, CDF note 2665; see also J.D. Lewis, J. Muller, J. Spalding and P. Wilson in "Proceedings of the Workshop on B physics at Hadron Accelerators", Snowmass, Colorado, June 21-July 2, 1993, eds. P. McBride and C.S. Mishra, p. 217.

[22] F. DeJongh and P. Sphicas, Phys. Rev. **D53**, 4930 (1996).

[23] The CDF Collaboration, *A Time–of–Flight System for CDF* Proposal submitted to the FNAL PAC, 28 March 1995.

[24] A. Spies and O. Schneider, *A Measurement of the B^+ and B^0 Lifetimes using Exclusive Decay Channels*, CDF note 2345.

[25] The CDF Collaboration, *SVXII Simulation Study and Upgrade Proposal*, CDF Note 1922, (see in particular Table 13).

[26] R. Aleksan, B. Kayser and P. Sphicas, in "Proceedings of the Workshop on B physics at Hadron Accelerators", Snowmass, Colorado, June 21-July 2, 1993, eds. P. McBride and C.S. Mishra, p. 291.

[27] E. Blucher, J. Cunningham, J. Kroll, F. Snider and P. Sphicas in "Proceedings of the Workshop on B physics at Hadron Accelerators", Snowmass, Colorado, June 21-July 2, 1993, eds. P. McBride and C.S. Mishra, p.309.

[28] I. Dunietz in Phys. Rev. **D52**, 3064 (1995).

[29] R. Fleischer and I. Dunietz, Fermilab-PUB-96/079-T, HEP-PH/9605220.

[30] A. Ali, V.M. Braun and H. Simma, Z. Phys. **C63**, 437 (1994); J.M. Soares, Phys. Rev. **D49**, 283 (1994); S. Narison, Phys. Lett. **B327** 354 (1994).

[31] E. Golowich and S. Pakvasa, UH-511-800-94; H. Y. Cheng, Phys. Rev. **D51**, 6228 (1995); D. Atwood, B. Blok and A. Soni, SLAC-PUB-6635.

[32] For a recent review, see J. Shigemitsu, *Lattice Gauge Theory: Status Report 1994* Proceedings of the XXVII International Conference on High Energy Physics, Glasgow, Scotland (1994).

[33] The industrious reader is advised to NOT attempt to form an average of these results as they are NOT all strictly independent. For the individual results see F. Bedeshci *et al., Measurement of the Mixing Parameter x_d via Time Evolution*, CDF note 2971; C. Gay *et al., A Measurement of the Time–Dependence of $B^0\bar{B}^0$ Oscillations using Low–p_T Electron–Muon Data*, CDF note 3791; O. Long *et al., Time Dependent B^0 Mixing in Inclusive Lepton Data using Jet Charge and Soft Lepton Flavor Tags*, CDF note 3810; F. DeJongh, P. Maksimovic and P. Sphicas, *An Investigation of Time–Dependent B^0 Mixing in Tagged Lepton+Charm Events*, CDF note 3644 (see also CDF note 3701.)

[34] D.J. Ritchie, J.E. Skarha and A. Zieminski, *Report of the Mixing Sub-Group of the δ Working Group*, Proceedings of the Workshop on B Physics at Hadron Accelerators, Snowmass, Colorado (1993); J. Skarha and A.B. Wicklund *Prospects for Measuring B_s Mixing at CDF*, Proceedings of the Workshop on B Physics at Hadron Accelerators, Snowmass, Colorado (1993).

[35] M. Paulini and M. Shapiro, *Study of x_s Reach for TDR*, CDF note 3693.

[36] K. Burkett and M. Paulini *Measurement of the Lifetime of the B_s^0 Meson from $D_s^+\ell^-$ Correlations*, CDF note 3519. See also, "Measurement of the B_s^0 Meson Lifetime." F. Abe *et al.*, Phys. Rev. Lett. **74** 4988 (1995).

[37] CDF SVX-II Upgrade Proposal, CDF Note No. 1922 (1993).

[38] J. Hagelin, Nucl. Phys. **B193**, 123 (1981); M.B. Voloshin *et. al* Sov. J. Nucl. Phys. **46**, 112 (1987).

[39] T.E. Browder and S. Pakvasa, UH 511-814-95. See also the recent discussion by M. Beneke, G. Buchalla and I. Dunietz, SLAC-PUB-7165, HEP-PH/9605259.

[40] I. Dunietz, Phys. Rev. **D51**, 2471 (1995).

[41] I. Bigi *et al.*, in "B Physics", 2nd edition, S. Stone editor.

[42] A.S. Dighe, I. Dunietz, H.J. Lipkin and J.L. Rosner, Phys. Lett. **B369**, 144 (1996).

[43] See Y. Grossman, WIS-96/13/Mar-PH, HEP-PH/9603244; M. Gronau and D. London, Technion-PH-96-37, HEP-PH/9608430, and Y. Nir, WIS-96/31/Jul-PH, HEP-PH/9607415 for recent discussions.

[44] The CLEO Collaboration, CLEO CONF 94-2.

[45] F. DeJongh and M. Shapiro, *A Proposal for Observing Radiative B Decays at CDF*, CDF Note 2570; K. Kordas *et al.*, *The CDF Penguin Trigger*, CDF Note 3771.

[46] E. Eichten and C. Quigg, Phys. Rev. **D49**, 5845 (1994).

[47] I. Dunietz, Phys. Lett. **B316**, 561 (1993).

[48] A. Ali, C. Greub, T. Mannel, *Proceedings of the ECFA Workshop on the Physics of the European B Meson Factory* (1993), 155. A. Ali and T. Mannel, Phys. Lett. **B264**, 447 (1991). Erratum, Phys. Lett. **B274**, 526 (1992).

[49] A. Ali, T. Mannel and T. Morozumi, Phys. Lett. **B273**, 473 (1991); B. Grinstein, M.J. Savage and M.B. Wise, Nucl. Phys. **B319**, 271 (1989); W. Jaus and D. Wyler, Phys. Rev. **D41**, 3405 (1991).

[50] A. Ali, G. Giudice and T. Mannel, *Towards a Model Independent Analysis of Rare B Decays*, Proceedings of the XXVII International Conference on High Energy Physics, Glasgow, Scotland (1994).

[51] M. Gronau and D. London, Technion-PH-96-37, HEP-PH/9608430.